CHAPTER 3

Heat Transfer Behavior of Flat Plate Having Spherical Dimple Surface

3.1 Introduction

In this chapter, the thermal characteristic of air flow over flat plate having spherical dimpled surface is studied. In addition, the effect of dimple arrangements, and dimple pitch will be included in this work. A total of 14 types of dimple surfaces are studied. The experiments are carried out with air stream flows over the heated surface with dimples. The heat transfer coefficient of dimple surfaces is investigated and reported.

3.2 Experimental setup and procedure

The schematic diagram of the experimental setup for heat transfer measurements is shown in Figure 3.1. The fluid used in the apparatus is air at room temperature, which is generated by an air blower. The stream air flows through the test section and flows over tested surface. In this experiment, the velocity of air stream was controlled by the frequency inverter with the controllable range of 1-5 m/s. The velocity of air stream was measured by four sets of hot wire anemometers with ±0.2 m/s accuracy. The anemometers were placed over the tested kit (outside velocity boundary layer was considered). The tested kit was placed next to the throttling device about 0.5H and flow straightener is far from tested kit 5H. The inlet temperature of air stream was measured by a four sets of T-type thermocouple with ±0.1 ^{o}C accuracy.

The test kit comprises tested plate and plate heater. Test plates are made from 1.5 mm thickness of acrylic which is depressed in any configurations of dimple. The iron powder was filled beneath the tested plate to avoid the space between the electric plate heater. All exterior of the test kit were insulated with three layers of 2.5 cm-thickness

glass wool insulation to minimize heat losses. The electric heater supplies a constant heat flux. The electrical power of the heater was controlled and regulated by a variac power supply. The T-type thermocouples are located between each layer to determine conduction losses.

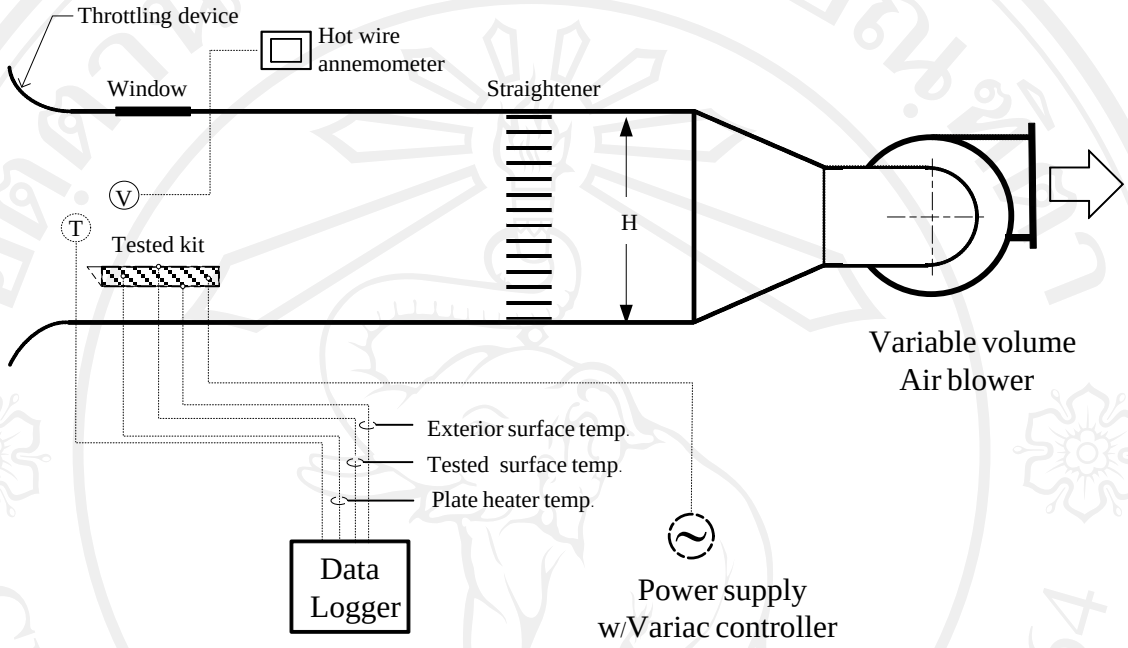

Figure 3.1 Schematic diagram of the experimental setup.

The surface temperature of flat plate was captured by infrared imaging camera with ±2 ^{o}C accuracy. The measuring procedure was adjusted in order to calibrate the surface temperature with T-type thermocouple with ±0.1 ^{o}C accuracy. The surface temperature is illustrated in color scale values. Contour plots of local surface temperature values have the resolution of 160×120 pixels and temperature values were exported to spread sheet form.

Figure 3.2 and 3.3 present the geometric details of the tested surface, including dimpled geometry. Dimples were employed in an inline and staggered array and table 3.1 lists the details of the test samples.

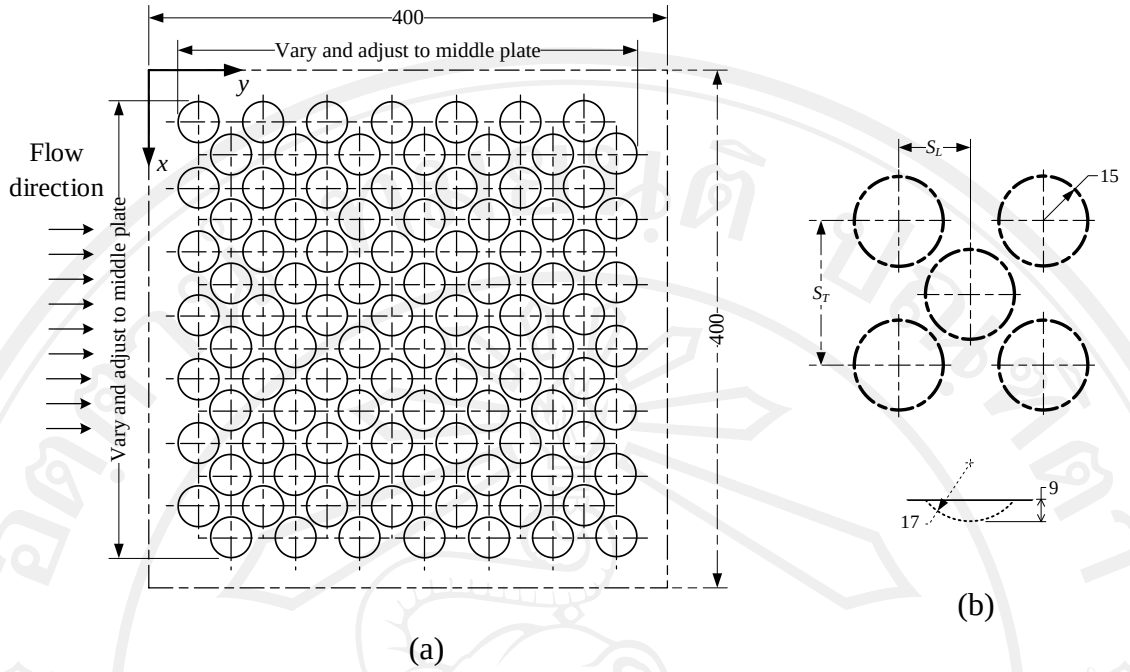

Figure 3.2 Details of: (a) dimpled-tested surface for staggered arrangement, and (b) individual dimple geometry. All dimensions are in mm.

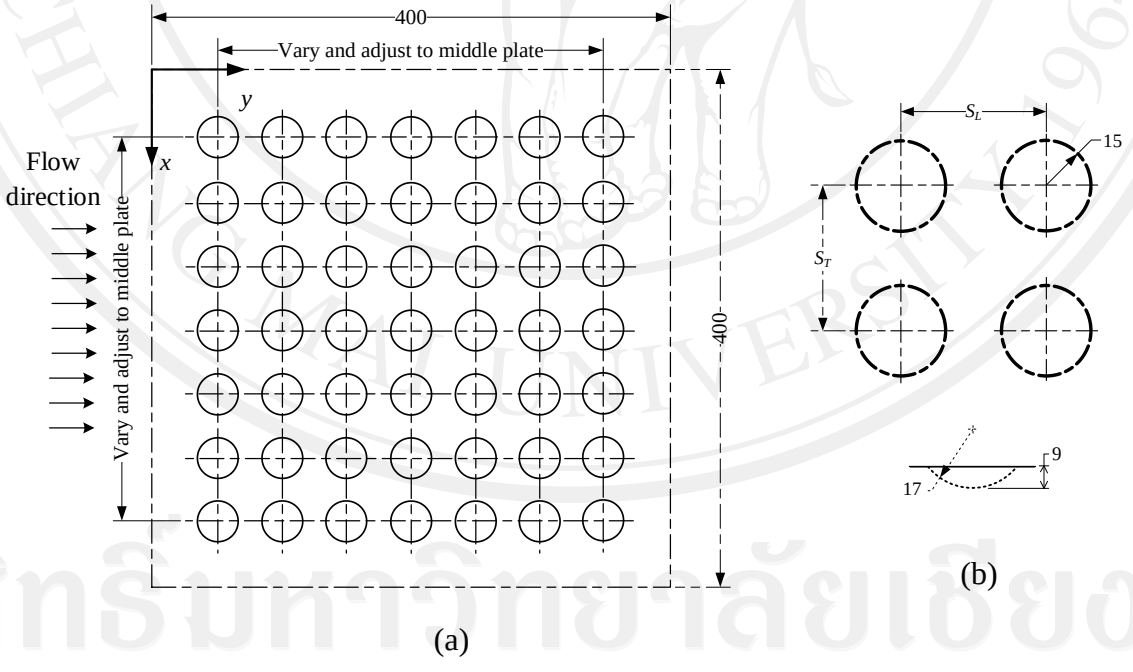

Figure 3.3 Details of: (a) dimpled-tested surface for inline arrangement, and (b) individual dimple geometry. All dimensions are in mm.

Table 3.1 Geometric dimensions of spherical dimple surface.

No	S_T (mm)	S_L (mm)	Arrangement	S_T/S_L
1	50	25.0	Staggered	2.00
2	50	30.0	Staggered	1.67
3	50	37.5	Staggered	1.33
4	60	25.0	Staggered	2.40
5	60	30.0	Staggered	2.00
6	60	37.5	Staggered	1.60
7	75	25.0	Staggered	3.00
8	75	30.0	Staggered	2.50
9	75	37.5	Staggered	2.00
10	36	36.0	Inline	1.00
11	36	45.0	Inline	0.80
12	36	60.0	Inline	0.60
13	45	45.0	Inline	1.00
14	60	45.0	Inline	1.33

3.3 Data reduction

The local heat transfer coefficient (h_x) of air flowing over flat plat with dimpled surface can be calculated from

$$h_x = q_s'' / (T_s - T_\infty) \tag{3.1}$$

where q_s'' is surface heat flux which is calculated from heat rate level at the tested surface divided by the total tested surface area (flat portions and dimples surface). T_s is the local surface temperature and T_α is the average air stream flowing over the tested plate respectively.

The average air side heat transfer coefficient (h) of tested surface is obtained by integrating over the area of tested surface as

$$h = \frac{1}{A_s} \int_{A_s} q_s'' / (T_s - T_\infty) dA_s \tag{3.2}$$

where A_s is tested surface area comprises flat portions and dimples surface.

The average Nusselt number (Nu_L) is the ratio of convection to pure conduction heat transfer which is given by

$$Nu_L = \frac{hL}{k_f} \tag{3.3}$$

where L is maxima stream-wise surface length comprises flat portions and dimples portions. k_f is the thermal conductivity of air stream.

It should be notice that the Reynolds number (Re_L) for this investigation is defined as

$$Re_L = \frac{\rho_f V_f L}{\mu_f}. \tag{3.4}$$

where ρ_f, V_f and μ_f are the density of air, the air frontal velocity and the dynamic viscosity of air stream respectively.

3.4 Results and discussion

3.4.1 Validation of the experiment

The validation of the experiment was conducted in this research. The heat transfer from plain flat plate was observed under the lamina flow air stream. The testing condition was the same as describe in the previous section. The result of this part was compared with the correlation presented by Incropera et al. (2007) for finding out the reliability and the accuracy of the experiment. This correlation is

$$Nu_L = 0.68\,\mathrm{Re}_L^{1/2}\,\mathrm{Pr}^{1/3}. \tag{3.5}$$

where Pr is the Prandlt number of air stream. Figure 3.4 show the comparison of Nusselt number from the experiment and that are computed by Eq. (3.5) at various air stream frontal velocity. It should be notice that the data from the experiment agrees very well with the model. Consequently, the experimental setup for this work is reliable and can be applied to the heat transfer experiment in case of the dimpled surface.

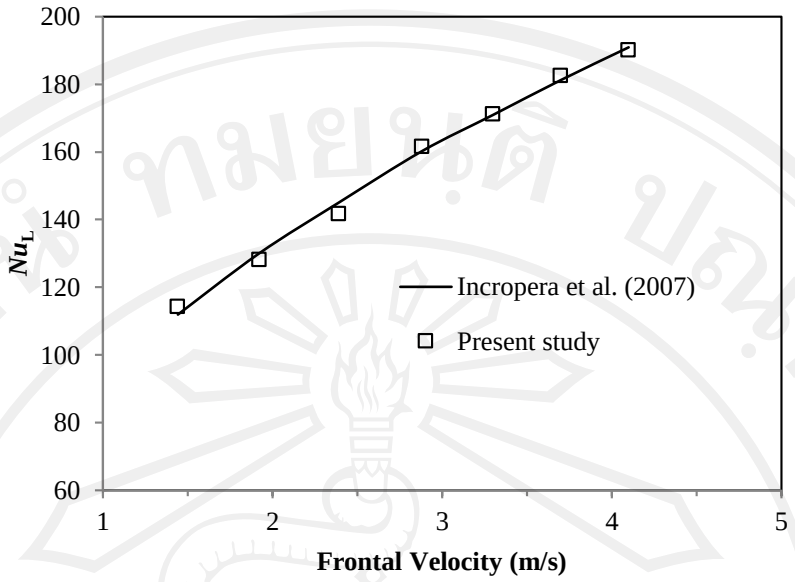

Figure 3.4 Comparison of the Nusselt number under the constant heat flux condition from the experimental and the model in case of plain flat plate.

3.4.2 Case of Staggered arrangement

3.4.2.1 Temperature distribution

In this study, the temperature distribution on the dimpled surface was observed by using the infrared imaging camera. The example of result is shown in Figure 3.5 which illustrates the temperature distribution along the tested surface of Geometric No.1. The bulk flow stream direction is from the left hand side. It is found that the dimples surface temperature is higher than that of plain surface. These results come from the recirculation of air stream in the dimpled. Moreover, it is found that in each dimpled, the temperature of upstream side is higher than that of the downstream. It means the heat transfer of upstream halve is lower than the downstream halve. Similar result was also observed by Mahmood et al. (2001). The lowest temperature of dimpled is observed near the diagonal and the downstream edge which the vortex of air stream is generated. Contradict to the results of dimples surface temperature, in case of flat portion, it is found that the surface temperature gradually increases along the downstream. This result

may be come from the increasing of air stream temperature along the plate length.

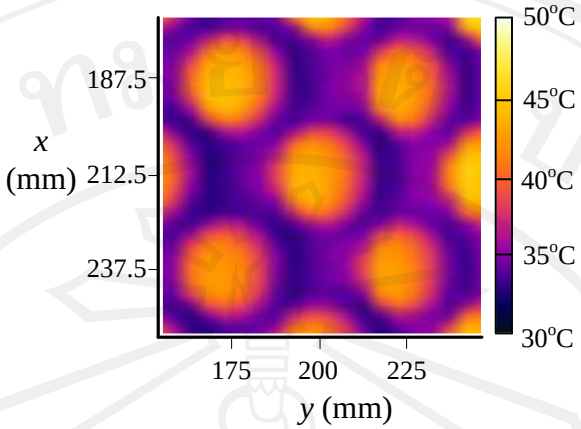

Figure 3.5 Temperature distributions of Geometric No.1 at frontal velocity = 4.1 m/s.

3.4.2.2 Effects of dimple pitch

In the case of staggered arrangement, there are nine samples as shown in Table 3.1. Figure 3.6 shows the effect of dimple pitch of the staggered arrangement of the air side heat transfer performance. Results are termed as heat transfer coefficient vs. frontal velocity. As seen in the Figure, heat transfer coefficient values are augmented at all frontal velocities and all dimple pitches compare to the flat plate. The Geometric No.2 yields the highest heat transfer coefficient around 21% better than the flat plate, and Geometric No.1, No.7 and No.9 yield the lowest heat transfer coefficient. It should be noted that higher heat transfer enhancement is observed in case of $S_T/S_L \leq 2.0$. Normally narrow S_T promotes the vortex of air stream; therefore, the heat transfer coefficient should be increased with the decreasing of S_T. However, the vortex generation of downstream dimpled row may be disturbed by that of upstream row. Therefore, the heat transfer augmentation of the shorter S_L may be lower than that of the longer. Consequently, the experimental result shows that higher heat transfer enhancement is observed in case of low S_T/S_L.

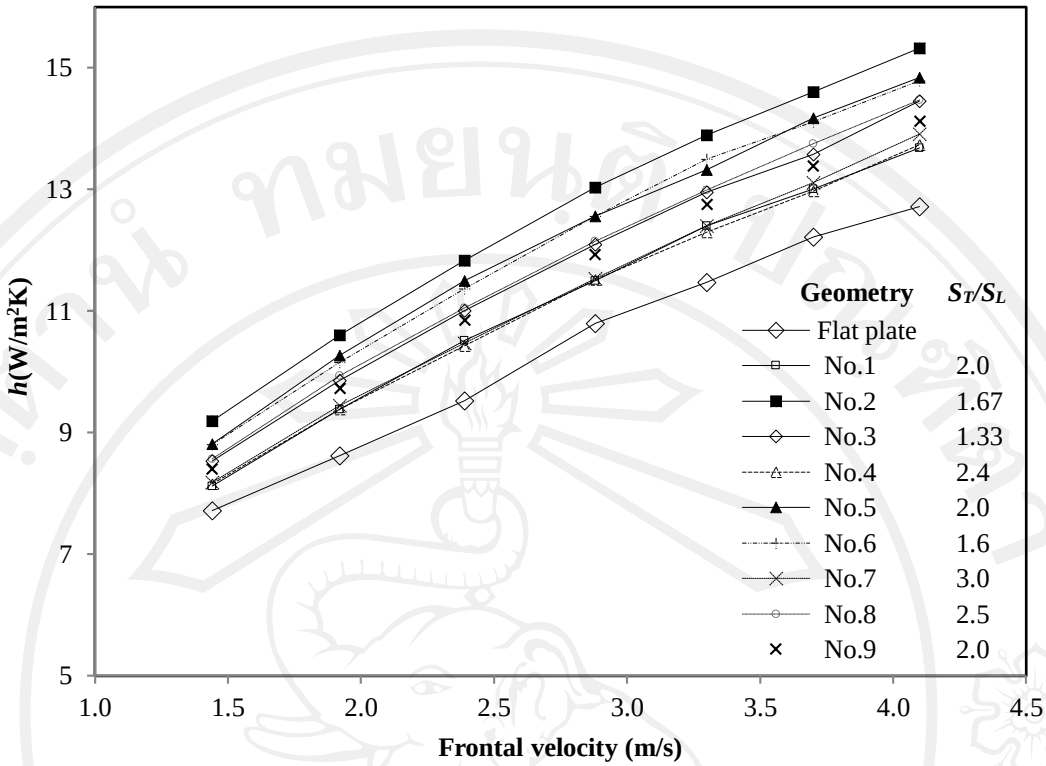

Figure 3.6 Effect of dimple arrangement on heat transfer coefficient for staggered arrangement.

The effects of varying dimple pitch are further illustrated by the results presented in Figure 3.7. The average heat transfer coefficient data in this Figure obtained by averaging local data in the span-wise direction. The frontal velocity of air stream is 4.1 m/s. The geometries 2, 5 and 8 are selected for observing the heat transfer phenomena. It should be noticed that y and h/h_0 are the distance along stream flow and the ratio of heat transfer coefficient in case of having dimpled and flat plate. It could be seen that at the dimpled surface, the heat transfer coefficient is extremely drops. This result comes from the recirculation of air inside the dimpled. However, the heat transfer coefficient ratio trends to increase with y direction. This result comes from the increasing of turbulent intensity with the increasing of dimpled row.

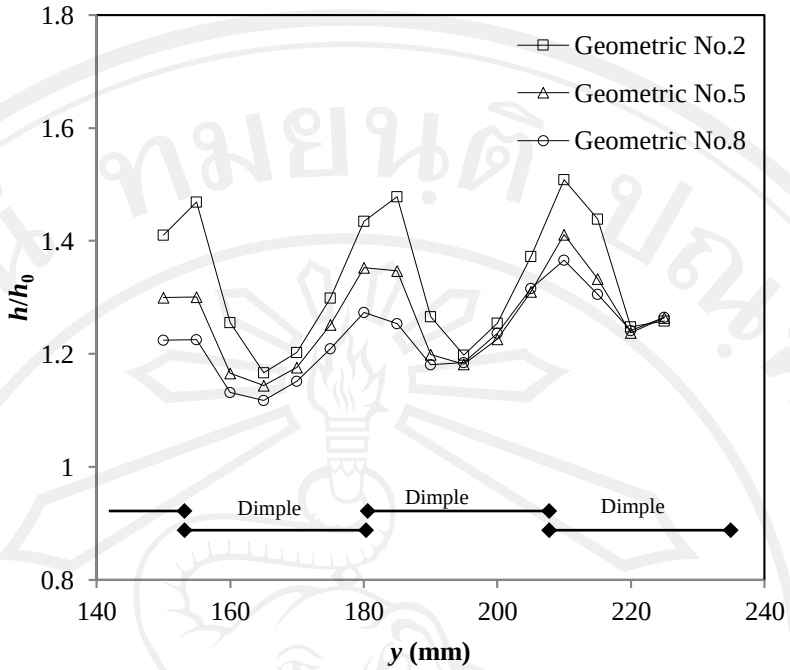

Figure 3.7 Span-wise averaged h/h_0, as dependent upon y at frontal velocity is 4.1 m/s in case of staggered arrangement.

3.4.3 Case of inline arrangement

3.4.3.1 Temperature distribution.

Figure 3.8 presents the temperature distribution on tested surface of Geometric No.11. The bulk flow direction is from left to right and the dimples are located nearly in each circular temperature distribution. The same temperature distributed trend with as staggered arrangement is found. The temperature values are highest in the upstream halves of the dimples and decrease progressively along the downstream of the dimples, which then become lowest near the diagonal and downstream edges.

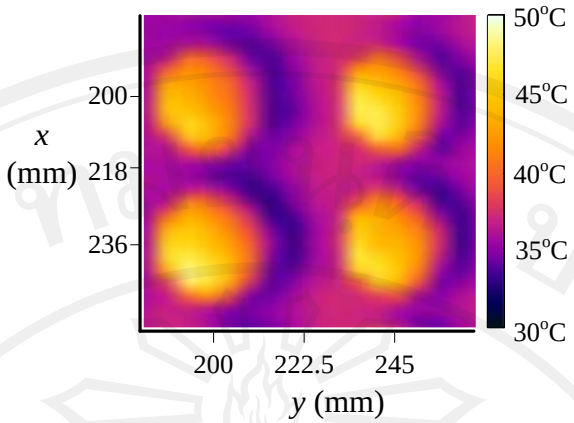

Figure 3.8 Temperature distributions of Geometric No.11 at frontal velocity = 4.1 m/s.

3.4.3.2 Effects of dimple pitch

In the case of inline arrangement, Results are termed as heat transfer coefficients vs. frontal velocity are shown in Figure 3.9. As seen in the Figure, heat transfer coefficient values are augmented at all frontal velocities and all dimple pitches, which the Geometric No.14 yield the highest values about 20% better than flat plate, and Geometric No.12 yields the lowest heat transfer coefficient. It should be noted that the pitch ratio (S_T/S_L) for this case is between 0.6 - 1.33 which lower than that of staggered case. From Figure 3.9, it should be noted that the higher S_T/S_L obtains the higher heat transfer coefficient.

Spatially-average heat transfer coefficient values are shown in Figure 3.10 for the frontal velocity equal to 4.1 m/s. The average data are obtained by averaging local data same as case staggered arrangement. As shown in the figure, the span-wise averaged h/h_0 values slightly increase along the downstream. These results are the same as staggered cases.

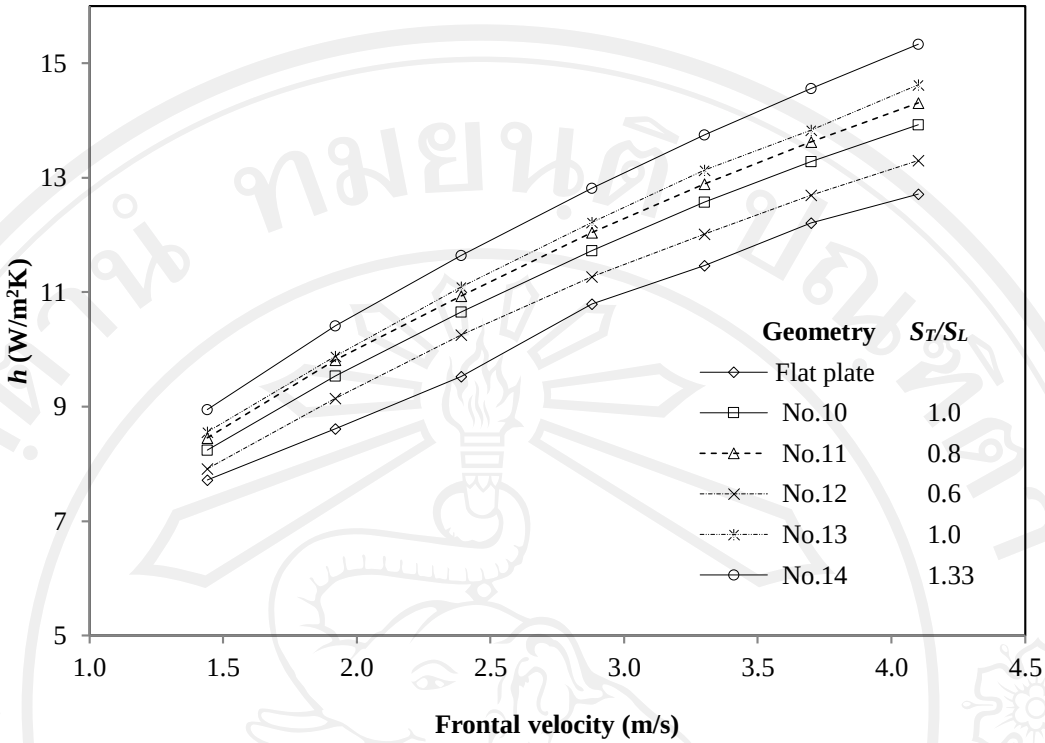

Figure 3.9 Effect of dimple arrangement on heat transfer coefficient for inline arrangement.

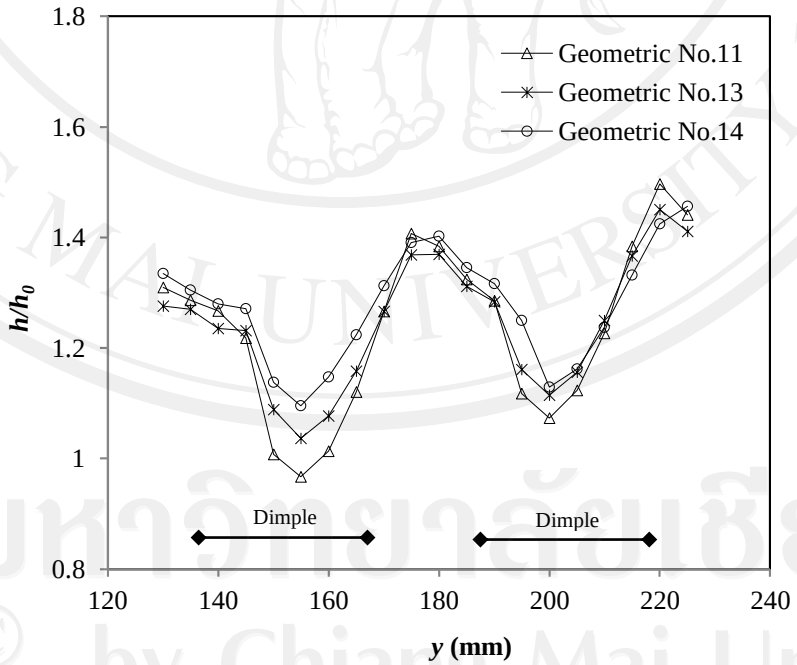

Figure 3.10 Span-wise averaged h/h_0, as dependent upon y at frontal velocity is 4.1 m/s in case of inline arrangement.

3.4.4 Empirical Correlation

From the previous results and discussions, the test data yield the complex behaviors about the heat transfer characteristics that no single curve can be expected to describe in both inline and staggered arrangements. For easier calculations, the multiple linear regression technique is performed to obtain the relevant correlations. The corresponding correlations are given as follows:

Correlation of the Nusselt numbers for the staggered arrangement:

$$\frac{Nu}{Nu_0} = 1.2341\left(\frac{S_L}{S_T}\right)^{0.0827}\left(\frac{S_T}{D}\right)^{0.0206} \tag{3.6}$$

Correlation of the Nusselt numbers for the inline arrangement:

$$\frac{Nu}{Nu_0} = 1.1853\left(\frac{S_T}{S_L}\right)^{0.1483}\left(\frac{S_T}{D}\right)^{0.0328} \tag{3.7}$$

Figure 3.11 shows the comparison of Nu/Nu_0 of the experimental results with the proposed correlations. For the Nusselt number correlations Eqs. (3.6) and (3.7) can predict 93.6% and 97% of the experimental data with ±5%. The standard deviation of the correlations Eqs. (3.6) and (3.7) are 3.36% and 1.69% respectively.

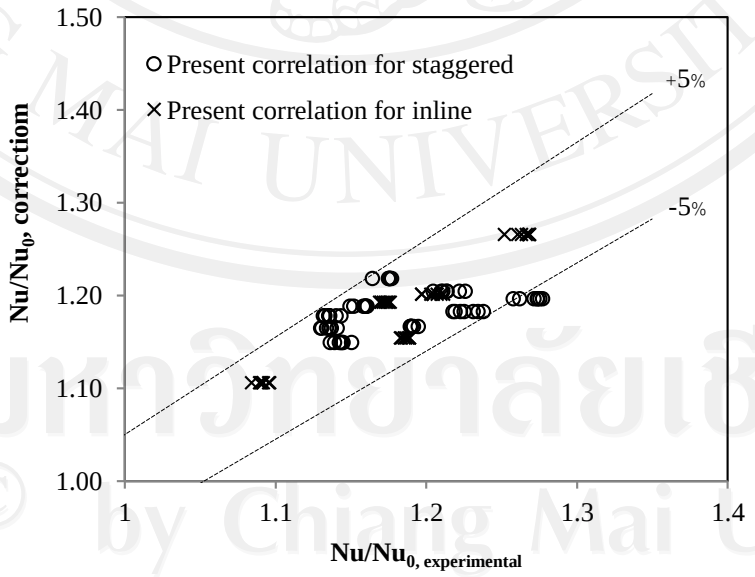

Figure 3.11 Comparison of heat transfer correlations with experimental data.

3.5 Summary and conclusion

The present study reports the heat transfer performance of air flow over the dimples surface. The effects of dimples pitch and dimples arrangement are examined. On the basis of previous discussions, the conclusions are made:

1) The air side heat transfer performance is augmented at all frontal velocity and all dimples pitch and arrangement. The heat augmentation is approximately 5-26%.

2) For staggered arrangements, the outstanding augmentation is found when the S_T/S_L lower than 2.0. However, in case of inline arrangement, the result show the highest heat transfer coefficient at S_T/S_L = 1.33.

3) Correlations of the present experiment in both staggered and inline arrangement are developed. The proposed correlations yield fairly good predictive ability against the present test data.

4) The vortexes generated by dimple are in three dimensions. The flow structure above the dimple should be further studies.